Tensin 3 is a new partner of Dock5 that controls osteoclast podosome organization and activity

Heiani Touaitahuata, Anne Morel, S Urbach, Julio Mateos-Langerak, Sylvain De Rossi, Anne Blangy

© 2016. Published by The Company of Biologists Ltd | Journal of Cell Science (2016) 129, 3449-3461 doi:10.1242/jcs.184622

RESEARCH ARTICLE

Tensin 3 is a new partner of Dock5 that controls osteoclast podosome organization and activity

Heiani Touaitahuata[1,2], Anne Morel[1,2], Serge Urbach[2,3], Julio Mateos-Langerak[2,4], Sylvain de Rossi[2,4] and Anne Blangy[1,2,*]

ABSTRACT

Bone resorption by osteoclasts is mediated by a typical adhesion structure called the sealing zone or actin ring, whose architecture is based on a belt of podosomes. The molecular mechanisms driving podosome organization into superstructures remain poorly understood to date, in particular at the osteoclast podosome belt. We performed proteomic analyses in osteoclasts and found that the adaptor protein tensin 3 is a partner of Dock5, a Rac exchange factor necessary for podosome belt formation and bone resorption. Expression of tensin 3 and Dock5 concomitantly increase during osteoclast differentiation. These proteins associate with the osteoclast podosome belt but not with individual podosomes, in contrast to vinculin. Super-resolution microscopy revealed that, even if they colocalize in the *x-y* plane of the podosome belt, Dock5 and tensin 3 differentially localize relative to vinculin in the *z*-axis. Tensin 3 increases Dock5 exchange activity towards Rac, and suppression of tensin 3 in osteoclasts destabilizes podosome organization, leading to delocalization of Dock5 and a severe reduction in osteoclast activity. Our results suggest that Dock5 and tensin 3 cooperate for osteoclast activity, to ensure the correct organization of podosomes.

KEY WORDS: Osteoclast, Podosome, Actin, Dock, Tensin, Adhesion

INTRODUCTION

Exacerbated by general population aging, osteoporosis has become a major health problem worldwide. In postmenopausal women, estrogen deficiency results in excessive bone loss, which is an important cause of osteoporosis. Various other conditions can also provoke osteoporosis, such as bone metastasis, disability and inflammation. Whereas excessive activity of osteoclasts is a common feature and hallmark of osteoporosis, it is caused by numerous diseases that have very distinct mechanisms (Weitzmann and Pacifici, 2006). Osteoclasts are myeloid cells and they represent the major bone-resorbing cells. Their mononuclear precursors belong to the monocyte and macrophage lineage, including bone marrow macrophages (BMMs). Monocyte precursors differentiate in response to the cytokines receptor activator of NF-κB ligand (RANKL) and M-CSF (macrophage colony-stimulating factor, also known as CSF1), to form pre-osteoclasts that ultimately fuse into polykaryons that are able to resorb mineralized matrices such as bone (Teitelbaum and Ross, 2003). To initiate bone resorption, osteoclasts undergo drastic morphological changes to assemble the actin ring or sealing zone. This adhesion structure is typical of osteoclasts. It is made of a belt of densely packed podosomes interconnected by an acto-myosin network. This belt surrounds the ruffled border, a highly convoluted region of the plasma membrane that secretes protons and proteases in contact with the bone. The ruffled border is the actual site where bone resorption takes place (Georgess et al., 2014; Touaitahuata et al., 2014a).

Among myeloid cells, osteoclasts have the unique ability to organize their podosomes into a belt, which is the backbone of the bone-resorbing apparatus. During the differentiation process, osteoclast podosome superstructures evolve from podosome clusters to podosome rings that expand and finally fuse into a belt (Destaing et al., 2003; Georgess et al., 2014; Touaitahuata et al., 2014a). This is accompanied by increasing levels of proteins necessary for podosome belt formation such as Src or Dock5 (Brazier et al., 2006; Vives et al., 2011). During bone resorption, podosome architecture is also dynamic owing to alternate resorption phases, when podosomes ensure efficient sealing of the osteoclast onto the bone matrix, and migration phases, during which podosomes disassemble to allow osteoclasts to migrate towards the next resorption area (Touaitahuata et al., 2014a). During their lifespan, osteoclasts undergo multiple resorption and migration cycles associated with extensive actin dynamics regulated by RhoGTPases (small GTPases form the Rho family), to assemble and disassemble podosomes (Saltel et al., 2004; Ory et al., 2008).

Podosomes are made of two distinct regions: the podosome core, characterized by the adhesion receptor CD44 and a very dense network of actin fibers running perpendicular to the substrate, and the podosome cloud. The latter contains two actomyosin networks: one that connects podosomes to the substrate through αvβ3 integrin, and one that interconnects podosomes (Linder and Wiesner, 2015). Several proteins were identified at the podosome cloud that contribute to the ability of osteoclasts to rearrange podosomes into the belt structure and build the bone-resorbing apparatus, including Dock5 (Vives et al., 2011), Vav3 (Faccio et al., 2005), vinculin (Fukunaga et al., 2014), FARP2 (Takegahara et al., 2010) and Pyk2 (Gil-Henn et al., 2007). Remodeling of the actin cytoskeleton through RhoGTPases is crucial for the regulation of podosomes organization in osteoclasts, but the regulatory mechanisms during podosome rearrangements that allow efficient osteoclast activity still remain unclear.

Dock5, an exchange factor for the small GTPase Rac, is a major regulator of podosome organization in osteoclasts. Dock5 drives the assembly of osteoclast podosomes into a belt, thereby controlling bone resorption by osteoclasts and, hence, bone mass *in vivo* in the developing, growing and adult mouse (Vives et al., 2011; Touaitahuata et al., 2014b). Moreover, the systemic injection of a small chemical compound inhibitor of Rac activation by Dock5

[1]CRBM, Centre de Recherche de Biochimie Macromoléculaire, CNRS UMR 5237, 34000 Montpellier, France. [2]Montpellier University, 34000 Montpellier, France. [3]Functional Proteomics Platform, Institut de Génomique Fonctionnelle, CNRS UMR 5203, 34000 Montpellier, France. [4]Montpellier RIO Imaging, Biocampus UMS3426 CNRS, 34000 Montpellier, France.

*Author for correspondence (anne.blangy@crbm.cnrs.fr)

A.B., 0000-0001-7043-0784

Received 15 December 2015; Accepted 25 July 2016

Journal of Cell Science (2016) 129, 3449-3461 doi:10.1242/jcs.184622

prevents bone loss in mice subjected to ovariectomy, collagen-induced arthritis or bone metastases, whereas bone formation by osteoblasts is preserved, thereby highlighting Dock5 as a novel target for the treatment of osteoporosis (Vives et al., 2015).

With Dock1 (also known as Dock180) and Dock2, Dock5 forms the Dock-A subgroup of the Dock family proteins, which contains 11 members. Proteins in the Dock-A subgroup are guanine nucleotide exchange factors specific for Rac, they contain an N-terminal SH3 domain that can bind the adaptor proteins Elmo1, Elmo2 and Elmo3, and a proline rich C-terminal domain that binds Crk proteins (Gadea and Blangy, 2014). Dock1 is ubiquitylated in response to growth factors, Crk or adhesion, and the protein is degraded by the proteasome. Binding of Dock1 to Elmo1 stabilizes Dock1 by preventing its ubiquitylation (Makino et al., 2006; Komander et al., 2008). However, nothing is known about the regulation of Dock5 itself.

To get a better understanding of the molecular mechanisms driving podosome organization allowing osteoclasts to degrade the bone, we sought to identify Dock5 partners in osteoclasts through proteomic analysis. This led us to the identification of tensin 3, an adaptor protein involved in the control of cell adhesion through the regulation of RhoGTPase activity (Cao et al., 2015). We show here that tensin 3 is a new regulator of bone resorption by osteoclasts, and that it activates Dock5 exchange activity towards Rac and regulates podosome organization.

RESULTS

Tensin 3 is a partner of Dock5 in osteoclasts

To get a better understanding of the molecular mechanisms that control the organization of podosomes in osteoclasts, we sought to identify partners of Dock5, an exchange factor for Rac, which controls the formation of the podosome belt and, hence, bone resorption by osteoclasts (Vives et al., 2011). We used RAW264.7 cells, a cellular model for osteoclasts, in order to obtain sufficient material for proteomic analyses. In RAW264.7-derived osteoclasts, Dock5 localizes to the podosome belt and these cells, when depleted for Dock5, have scattered podosomes and are unable to degrade mineral matrices, similar to what is observed for osteoclasts derived from BMMs (Vives et al., 2011). To identify Dock5-binding partners in osteoclasts, we applied a label-free mass spectrometry approach (spectral count). RAW264.7 cells stably expressing GFP-fused Dock5 or GFP alone were differentiated into osteoclasts and GFP proteins were affinity purified from total cell extracts. The purified complexes were resolved by SDS-PAGE and analyzed by nano liquid chromatography tandem mass spectrometry (LC-MS/MS). MS/MS spectra of tryptic peptides were used for protein identification. Tryptic peptide sequence analysis identified 2534 different proteins in SwissProt or TrEMBL databases (Table S1). For each protein, we determined the ratio between the average number of peptide spectrum match (PSM) in the GFP–Dock5-associated complexes and in the GFP-associated complexes, which we plotted against the number of peptides identified (Fig. S1). This clearly highlighted Elmo1 (84 kDa) and tensin 3 (155 kDa) as the most abundant partners of Dock5 based on PSM ratios. The PSM ratios were, respectively, 38.67 and 23.67 for Elmo1 and tensin 3 and protein coverage, respectively, was 31.91% and 18.75% (Fig. 1A). The identification of Elmo1, a known regulator of the stability of Dock-family exchange factors (Makino et al., 2006; Komander et al., 2008), was a good indication of the relevance of our approach to identify Dock5 partners in osteoclasts.

Given that it has recently been shown that tensin 3 is involved in the regulation of RhoGTPase activity (Cao et al., 2015) and that Dock5 is a major activator of Rac in osteoclasts (Vives et al., 2011), but no information was available regarding a potential functional relationship between tensin 3 and Dock proteins, we thought to investigate the function of Dock5 interaction with tensin 3 in osteoclasts. Tensin 3 is related to tensin 1 and tensin 2. Among the 18 tryptic peptides we identified for tensin 3, only one was common to the three tensins (Table S2). By contrast, we did not find any peptide specific for tensin 1 or tensin 2 in the proteomics, which unambiguously identifies tensin 3 as the partner of Dock5. Tensin 3 expression levels were very high in osteoclasts as compared to NIH3T3 fibroblastic cells, whereas tensin 1 was expressed at very low levels in osteoclasts and the levels of tensin 2 were equivalent in osteoclasts and NIH3T3 cells (Fig. S2A). As we did not find any specific peptide for tensin 2, this suggests a specific interaction between Dock5 and tensin 3 relative to other tensins in osteoclasts.

To verify the mass spectrometry data obtained with RAW264.7 cells expressing GFP–Dock5, we moved to bone-marrow-derived primary osteoclasts. We performed immunoprecipitation on osteoclast whole-cell extracts using tensin 3-specific antibodies, and found that Dock5 was present in the affinity complex (Fig. 1B). We found that the expression of tensin 3 protein increased during M-CSF and RANKL-induced osteoclast differentiation from bone marrow macrophages (BMMs), in parallel to that of Dock5 (Fig. 1C,D). The association of tensin 3 with some of its partners has been shown to rely on tyrosine phosphorylation by Src (Qian et al., 2009). We investigated the effect of Src-family kinase inhibitor PP2 on the complex between Dock5 and tensin 3 in osteoclasts. Treatment of osteoclasts for 60 min with 10 µM PP2 provoked the expected dephosphorylation of the Src target vinculin at Y1065 (Fig. 1E). Nevertheless, the association of tensin 3 with Dock5 remained unaffected, as shown by co-immunoprecipitation (Fig. 1E). Therefore, Src activity does not seem to be necessary for the interaction between tensin 3 and Dock5 in osteoclasts. By contrast, tensin 3 also interacted with β3 integrin in osteoclasts, which was inhibited by PP2 treatment (Fig. 1F). This is consistent with tensin and talin binding to the tail of β-integrin, and phosphorylation by Src favoring the binding of tensin by displacing talin (McCleverty et al., 2007). Of note, we did not find any component of the integrin complex among Dock5 partners, suggesting that there are two pools of tensin 3 in osteoclasts, bound either to Dock5 or to β3 integrin.

These results show that Dock5 and tensin 3 accumulate during RANKL-induced osteoclast differentiation and are part of the same protein complex in osteoclasts.

Dock5 and tensin 3 colocalize during podosome belt formation

We further analyzed in more detail the localization of endogenous Dock5 and tensin 3 during osteoclast differentiation by confocal microscopy (Fig. 2). Interestingly, both proteins exhibited the same dynamic pattern of association with podosome structures. When podosomes organized as clusters, which is considered the early step of podosome patterning in osteoclasts (Destaing et al., 2003), we did not find any enrichment of Dock5 and tensin 3 at podosomes. As expected, vinculin was present as ring-shaped structures at the periphery of podosome F-actin cores, defined as the podosome cloud (Fig. 2A,D,E). When podosomes assembled into rings, Dock5 and tensin 3 started to enrich there. In such structures, both proteins were present at the podosome core and at the podosome cloud, respectively labeled with actin and vinculin (Fig. 2B,D,E). Finally, when podosomes formed a well-defined peripheral belt in osteoclasts, characterized by F-actin label lined by two vinculin

Journal of Cell Science (2016) 129, 3449-3461 doi:10.1242/jcs.184622

A

Accession (a)	Gene	MW (kDa)	Mean DOCK5 PSM (b)	Mean GFP PSM (c)	PSM pseudo Ratio	Coverage (%)
Q8BPU7	**Elmo1**	83.9	19.33	0.50	**38.67**	31.91
Q5SSZ5	**Tns3**	155.5	23.67	1.00	**23.67**	18.75
B2RY04	**Dock5**	214.3	56.00	3.00	**18.67**	32.28

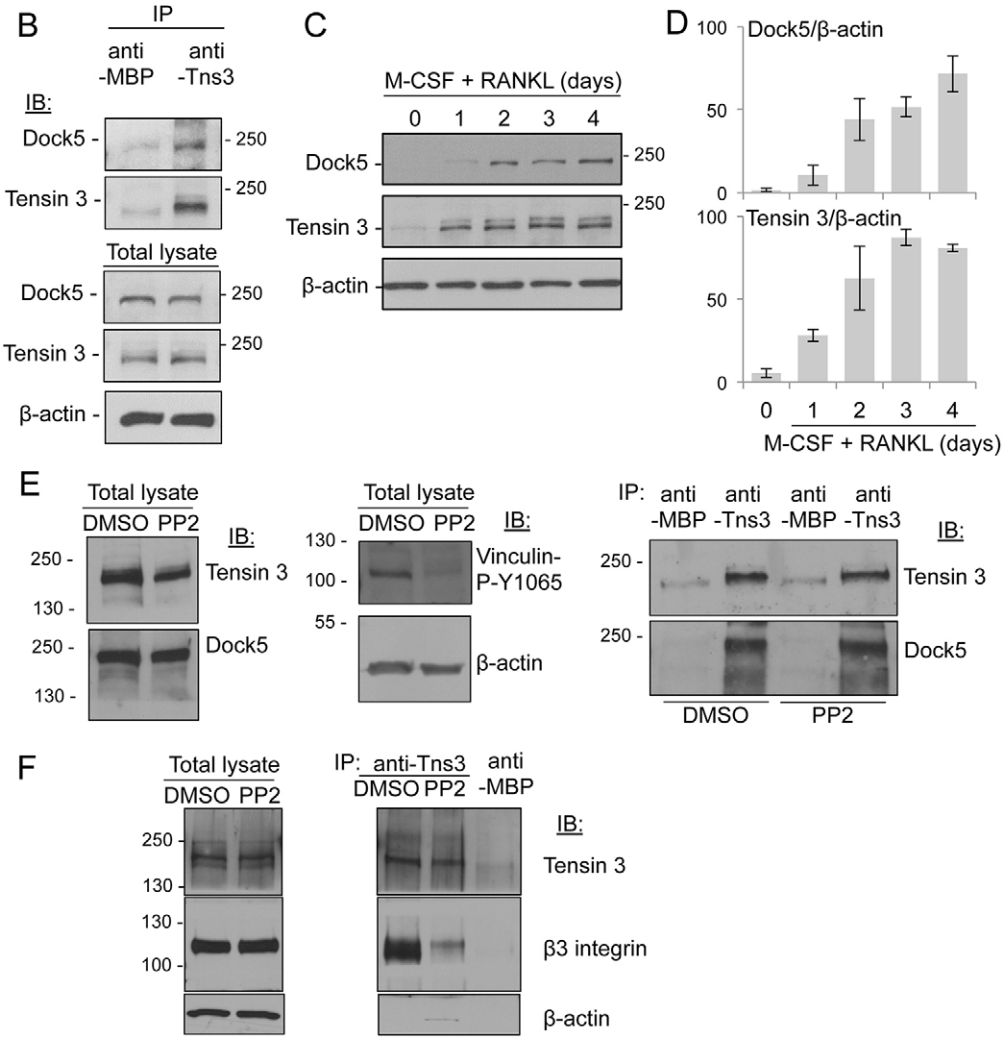

Fig. 1. Tensin 3 is a partner of Dock5 in osteoclasts. (A) Dock5 partners as determined by a mass-spectrometry-based comparison between proteins associated with GFP–Dock5 and GFP in osteoclasts derived from RAW264.7 cells. a, Uniprot reference; b, average peptide spectrum matches in GFP–Dock5 immunoprecipitate, *n*=3 independent osteoclast preparations; c, average peptide spectrum matches in GFP immunoprecipitate, *n*=2 independent osteoclast preparations. (B) Immunoprecipitation (IP) with antibodies against tensin 3 (Tns3) or maltose-binding protein (MBP) from primary osteoclast lysates, followed by western blotting (IB) to reveal endogenous Dock5 in tensin 3 immunoprecipitates, with β-actin used as a loading control. (C) Expression of Dock5 and tensin 3 in mouse BMM-derived osteoclasts determined after growth in M-CSF and RANKL for the indicated period of time, with β-actin used as a loading control. (D) Bar graphs showing the mean±s.e.m. values from densitometric analyses of the levels of Dock5 or tensin 3 normalized to β-actin at the indicated number of days in culture from three independent primary osteoclast preparations. (E,F) Immunoprecipitation, as in B, and western blot (IB) analyses of lysates from primary osteoclasts treated (PP2) or not (DMSO) with 10 µM PP2 for 1 h.

strips, Dock5 and tensin 3 colocalized with vinculin but not with the actin-dense podosome cores (Fig. 2C–E). The localization of endogenous Dock5 at the podosome belt of primary osteoclasts was similar to the localization of GFP–Dock5 expressed in RAW264.7-derived osteoclasts (Vives et al., 2011). Simultaneous labeling of Dock5 and tensin 3 in BMM-derived osteoclasts confirmed their colocalization at the podosome belt (Fig. 3A,B).

This shows that Dock5 and tensin 3 follow a similar dynamic localization during osteoclast podosome patterning. They are not associated with isolated podosomes, but specifically enrich in podosome superstructures and are associated with osteoclast podosome belt.

Super-resolution microscopy reveals differential localization of Dock5, tensin 3 and vinculin at the podosome belt

To get better insights into the localization of Dock5, tensin 3 and vinculin at the podosome belt, where they appear to colocalize by classical confocal microscopy, we moved to super resolution microscopy by performing 3D-structured illumination microscopy (3D-SIM) (Fig. 4). This approach confirmed the colocalization of Dock5, tensin 3 and vinculin at the podosome belt in the *x*-*y* plane (Fig. 4A,B), whereas we observed differential localization of the three proteins in the *z*-axis (Fig. 4C–H). In plane-by-plane analyses (Fig. 4C,D), as well as images of orthogonal *x*-*z* projections along the *y*-axis (Fig. 4E,F, top two panels), vinculin appeared to stand below Dock5 along the *z*-axis (Fig. 4C,E) whereas tensin 3 and Dock5 seemed to be more colocalized, with Dock5 standing preferentially in the upper part of the tensin 3 area (Fig. 4D,F). This was confirmed by the analysis of the profiles along the *z*-axis: both vinculin and tensin 3 staining began below that of Dock5 (line graphs in Fig. 4E,F). Interestingly, whereas 54.6% of Dock5 overlapped with vinculin and 59.6% of vinculin overlapped with Dock5 (Fig. 4G,H), as much as 85.8% of Dock5 was found to colocalize with tensin 3 and 68.6% of tensin 3 to colocalize with Dock5 (Fig. 4G,H).

These observations show that Dock5, tensin 3 and vinculin are present in the same area of the podosome belt relative to the plane of

Journal of Cell Science (2016) 129, 3449-3461 doi:10.1242/jcs.184622

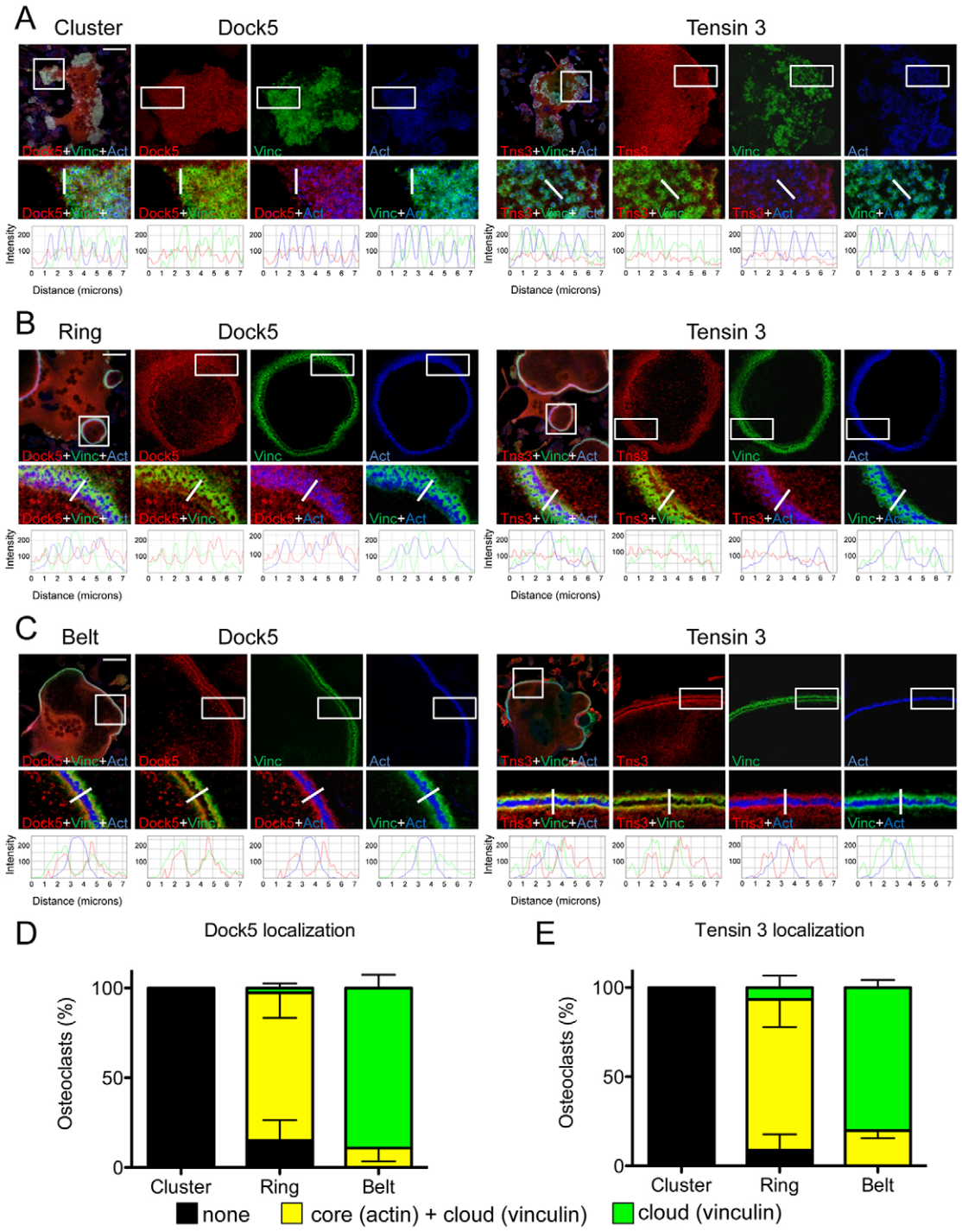

Fig. 2. Dynamic colocalization of Dock5 and tensin 3 during osteoclast podosome organization. (A–C) Podosome clusters, rings and belts in representative BMM-derived osteoclasts differentiated on glass coverslips and stained for Dock5 (left panels) or for tensin 3 (Tns3) (right panels) (red), and for vinculin (Vinc, green) and actin (Act, blue). Top left panels show the full field overlay of the three labels, with the square-boxed area magnified and shown for each label in adjacent panels. Scale bars: 50 µm. Bottom panels are magnifications and overlays of the rectangle-boxed areas above. Below are the corresponding fluorescence intensity profiles of Dock5 or tensin 3 (red lines), vinculin (green lines) and actin (blue lines) across the structures of interest (thick white lines in above panels). (D,E) Bar graphs showing the mean±s.e.m. percentage Dock5 (D) or tensin 3 (E) at podosomes in least 100 osteoclasts per category from two independent experiments. Yellow bars, the protein is in both the cloud and the core, the staining encompasses both vinculin and actin areas; green bars, the protein is only in the cloud, staining localizes only in the vinculin area; black bars, no specific accumulation at podosomes.

the substratum but have distinct distribution along the height of this adhesion structure. Vinculin was closer and Dock5 further away from the substratum whereas tensin 3, which can associate with both Dock5 and integrin β3 (Fig. 1E,F), exhibited a broader distribution.

Tensin 3 and Dock5 interact through their N-terminal domains

We next investigated the regions of interaction between Dock5 and tensin 3 using various deletion mutants expressed in 293T cells

Journal of Cell Science (2016) 129, 3449-3461 doi:10.1242/jcs.184622

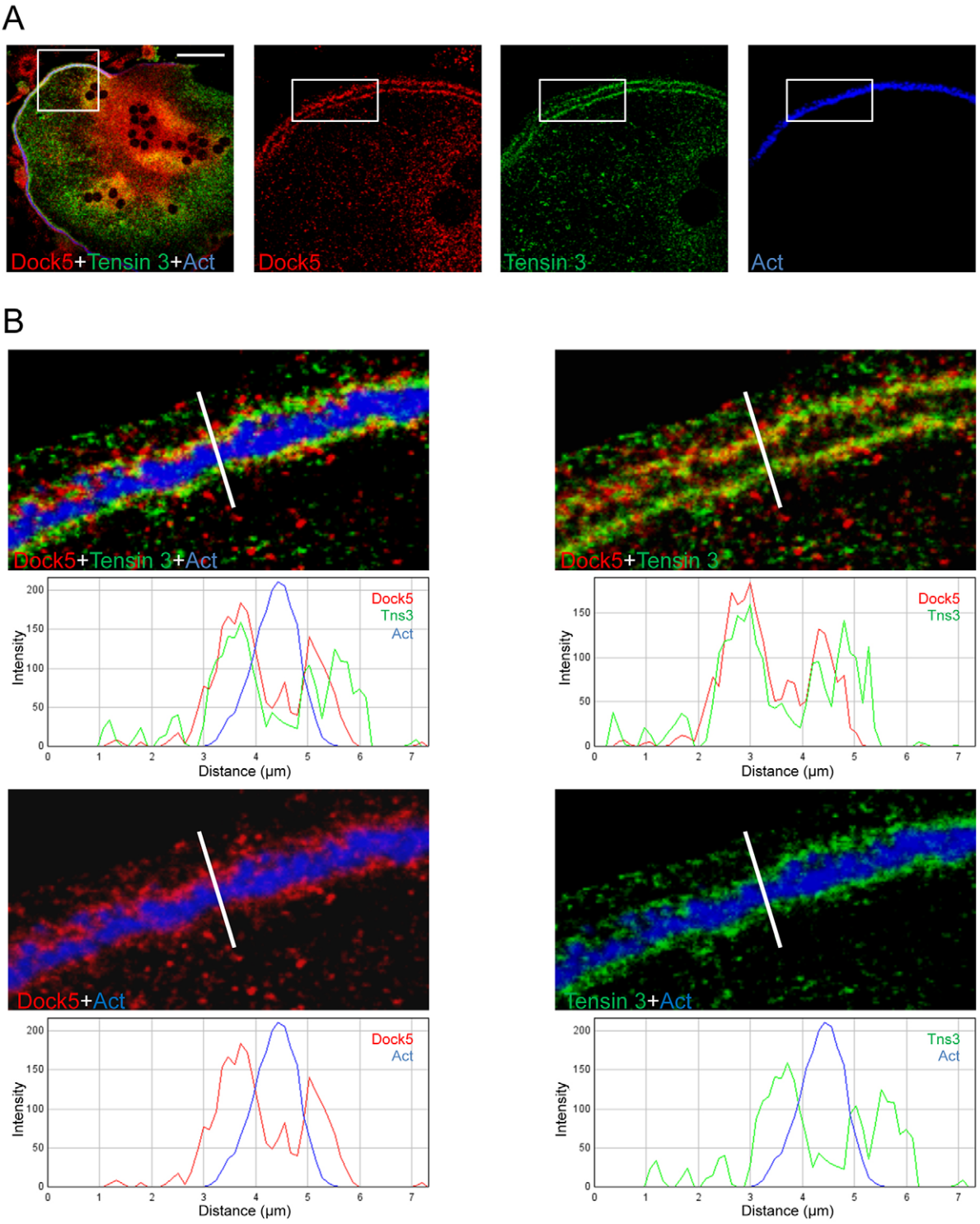

Fig. 3. Colocalization of Dock5 and tensin 3 at the podosome belt. (A) Confocal images of a representative BMM-derived osteoclast differentiated on glass coverslips and stained for Dock5 (red), tensin 3 (green) and actin (Act, blue). The left panel shows the full field overlay of the three labels, with the square-boxed area magnified and shown for each label in adjacent panels. Scale bar: 50 μm. (B) Magnification and overlay of the rectangular-boxed area in A, with fluorescent intensity profiles of Dock5 (red lines), tensin 3 (green lines) and actin (blue lines) across the podosome belt (white lines in above panels). This result is representative of at least 100 osteoclasts in three independent primary osteoclast differentiations.

(Fig. 5A). Co-immunoprecipitation experiments revealed that Dock5 was able to bind to tensin 3 with a deletion of its C-terminal SH2 and phosphotyrosine-binding (SH2-PTB) domain (ΔCter) and to its N-terminal actin-binding domain (ABD) (Lo, 2004) (Fig. 5B). By contrast, Dock5 did not bind the central domain (MID) and the C-terminal SH2-PTB domain (Cter) of tensin 3 (Fig. 5B). This suggests that the ADB domain of tensin 3 mediates its interaction with Dock5. By contrast, we found that deletion of Dock5 N-terminal SH3 domain did not affect the binding of tensin 3, this domain being necessary for Dock5 binding to Elmo1

Journal of Cell Science (2016) 129, 3449-3461 doi:10.1242/jcs.184622

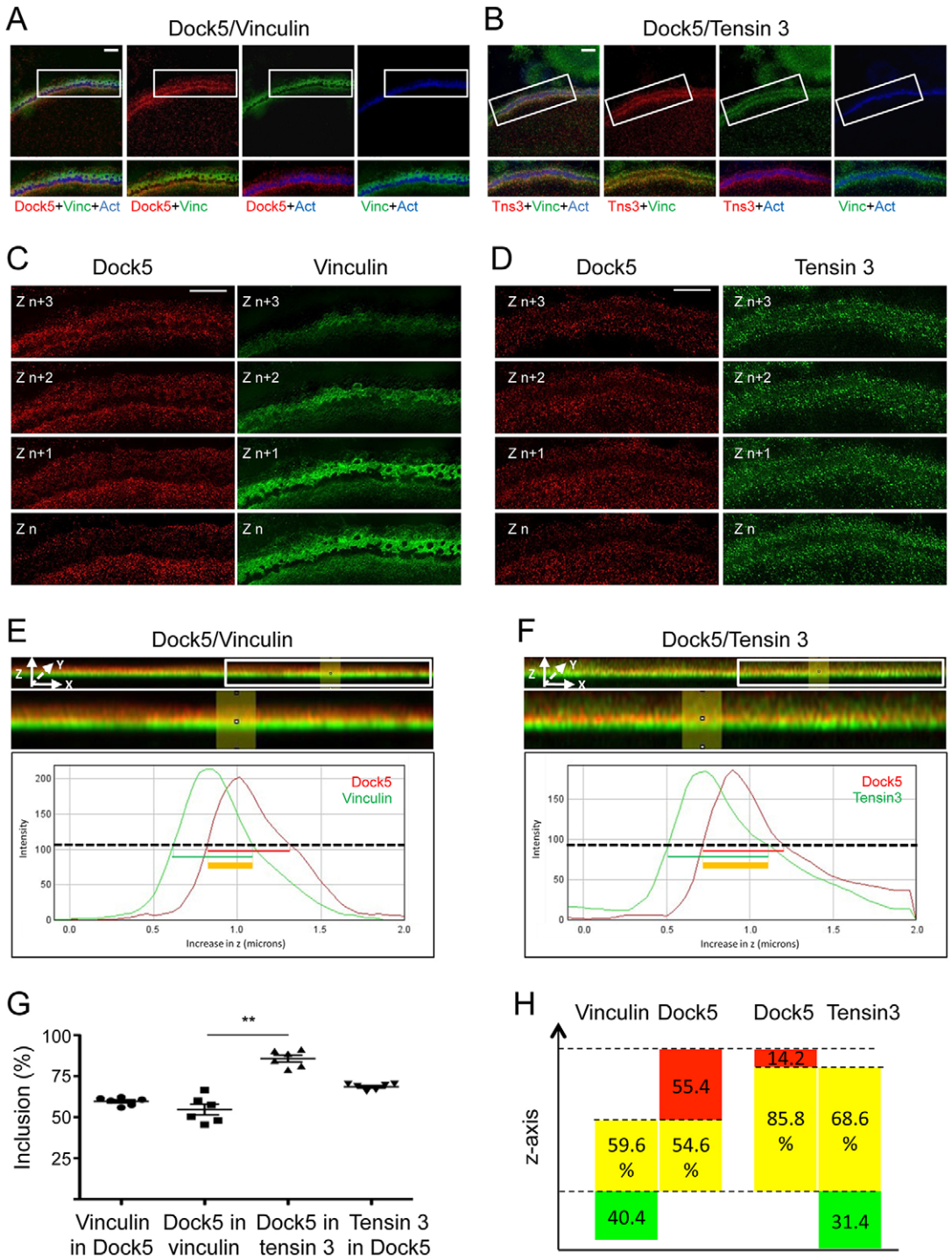

Fig. 4. 3D-structured illumination microscopy reveals differential localization of Dock5, tensin 3 and vinculin in the *z*-axis at the podosome belt. Primary osteoclasts differentiated on glass coverslips and stained for Dock5 (red), actin (Act, blue) and vinculin (Vinc, green in A, C and E) or tensin 3 (Tns3, green in B, D and F). Images were acquired in the podosome belt area by 3D-SIM super-resolution microscopy, as 18-plane *z*-stacks encompassing 2 µm from the coverslip plane (graph lines in E and F). (A,B) Top panels, *z*-stack projection of a representative area of the podosome belt, with boxed areas magnified and superimposed for the indicated labels in the bottom panels. Scale bars: 5 µm. (C,D) Four consecutive *z* planes from A and B, showing Dock5 (red) and vinculin or tensin 3 (green, respectively, in C and D). Scale bars: 13 µm. (E,F) Top images correspond to side views of the complete 18-plane *z*-stacks of A and B after projection along the *y*-axis, with magnification of the boxed area below. Yellow color shows the overlay between the red and green labels. Line graphs are representative fluorescent intensity profiles along the *z*-axis, between z=0 (bottom) and z=2 µm (top), of Dock5 (red curve, E and F) and vinculin or tensin 3 (green curve, respectively, E and F). Red and green horizontal lines show protein spanning measured at 50% of the maximum fluorescence signal intensity with the region of overlap as a thick yellow line. (G) Scatter plot graph (with the mean±s.e.m. marked) showing the percentage of vinculin overlapping with Dock5, of Dock5 overlapping with vinculin, of Dock5 overlapping with tensin 3 and of tensin 3 overlapping with Dock5 in six different osteoclasts, determined from line graphs as exemplified in E and F. ***P*<0.01 (Mann–Whitney test). For each osteoclast, the overlap percentage was defined as the average overlap at three randomly chosen positions within a representative region of the podosome belt as exemplified in A–F. (H) Scheme to recapitulate the position of Dock5 relative to vinculin or to tensin 3 in the *z*-axis, with yellow boxes being the average inclusion percentages determined in G.

Journal of Cell Science (2016) 129, 3449-3461 doi:10.1242/jcs.184622

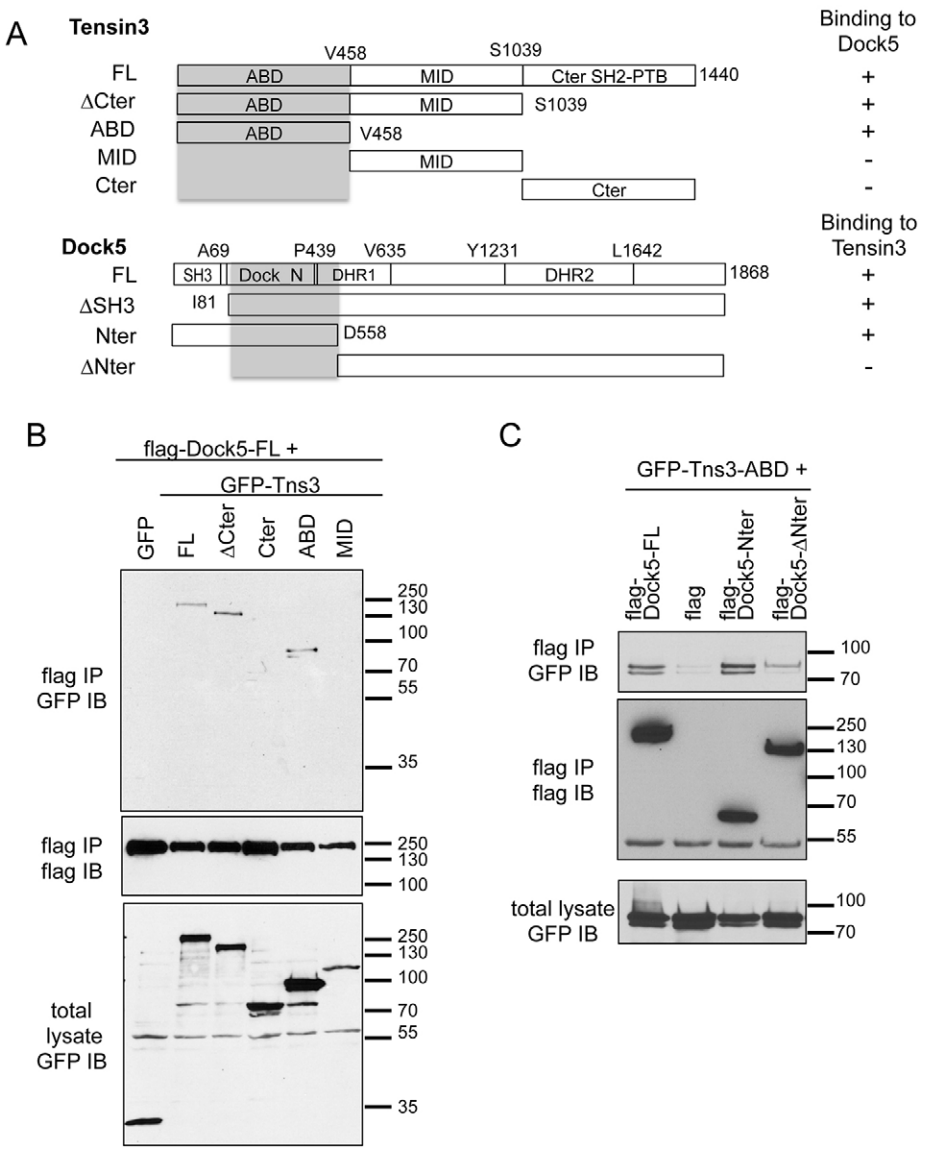

Fig. 5. Determination of the interaction domains between tensin 3 and Dock5. (A) Map of the different domains of tensin 3 and Dock5 with the interaction domains highlighted in gray. (B,C) HEK293T cells expressing the indicated constructs were immunoprecipitated with anti-Flag antibodies (flag IP) and western blotting was performed for GFP (GFP IB) or Flag (flag IB) to detect the proteins of interest. This analysis identifies the region from I81 to D558 of Dock5 as able to interact with tensin 3 ABD.

C-terminal domain (Fig. S3A,B). Of note, Elmo1 expression did not affect the interaction between Dock5 and tensin 3 (Fig. S3A). Further deletion mutant analyses indicated that the binding site of tensin 3 ABD on Dock5 was in the region between amino acids 81 and 558 of Dock5, corresponding to the uncharacterized Dedicator of cytokinesis, N-terminal domain (Dock_N, IPR032376), which lies between the SH3 and the DHR1 domains (Fig. 5C). These results indicate that the ABD domain of tensin 3 and the Dock_N domain of Dock5, independently from its SH3 domain, mediate the interaction between the two proteins.

Tensin 3 stimulates Dock5 exchange activity towards Rac

Consistent with what was reported for Dock180 (Lu et al., 2005), we found that the amino-terminal SH3 domain of Dock5 inhibited its exchange activity: deletion of the SH3 domain of Dock5 strongly increased its ability to activate endogenous Rac in HEK293T cells, as shown by pulldown assays (Fig. S3C–E). Tensins were shown to exert a complex effect on RhoA GTPase-activating protein (GAP) Dlc1: on one hand, binding of tensin ABD to Dlc1 has been shown to relieve the intramolecular inhibition of the GAP (Cao et al., 2012); however, on the other hand, tensins have been reported to inhibit Dlc1, in a manner that involves the C2, the SH2 and the PTB domains of tensin (Shih et al., 2015). Thus, we investigated a potential effect of tensin 3 on the exchange activity of Dock5. We observed that co-expression of tensin 3 significantly increased the activation of Rac by Dock5 in HEK293T cells, whereas expression of tensin 3 alone had no effect on Rac activity (Fig. 6A,B). We then performed Rac pulldown assays upon co-expressing Dock5 with different fragments of tensin3. In contrast to the full-length protein, we did not find any modification of Dock5 activity in the presence of the tensin 3 ΔCter fragment, which can interact with Dock5. The overexpression of tensin 3 ABD or Cter strongly impaired cell adhesion, which prevented making reliable Rac pulldown assays (data not shown). This suggests that binding of the ABD to the N-terminal region of Dock5 is not sufficient to stimulate its activity and that more complex mechanisms are involved, possibly relying on structural reorganizations and/or other partners of tensin 3.

These results suggest that the association of tensin 3 with Dock5 increases the activity of the exchange factor towards the GTPase Rac.

Journal of Cell Science (2016) 129, 3449-3461 doi:10.1242/jcs.184622

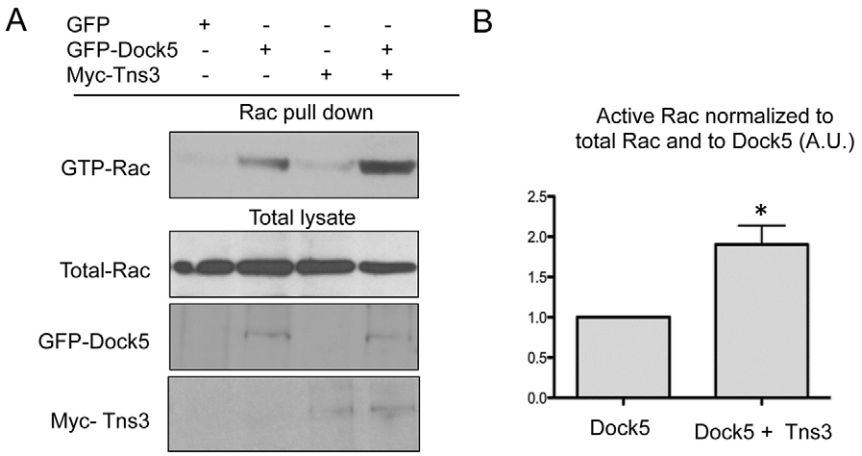

Fig. 6. Tensin 3 can relieve Dock5 intramolecular inhibition. (A) Representative pulldown assay to determine endogenous Rac activation (GTP-Rac) in HEK293T cells expressing GFP or GFP–Dock5 (Dock5) and/or Myc-tagged tensin 3 (Tns3), with levels of endogenous Rac, and GFP–Dock5 and Myc–Tns3 also shown for the total cell lysates. (B) Bar graph showing the densitometric analysis (mean±s.e.m.) of active Rac normalized to the levels of total Rac and total Dock5 in HEK293T cells expressing Dock5 with or without tensin 3, from six independent experiments as exemplified in A. *P<0.05 (Wilcoxon rank test).

Tensin 3 is necessary for bone resorption and it regulates RhoGTPase activity in osteoclasts

As tensin 3 localizes at the podosome belt, we hypothesized that it could play a role in podosome organization and bone resorption. To explore this, we tested the effect of tensin 3 depletion by transfecting small interfering RNAs (siRNAs) in BMM-derived osteoclasts (Fig. 7A). Tensin 3 depletion did not appear to affect the levels of Dock5 in osteoclasts (Fig. 7A). As compared to control siRNA targeting luciferase, the transfection of tensin 3 siRNA decreased the number of osteoclasts with a podosome belt, defined as cells presenting vinculin as a double line label flanking the actin staining of the podosome cores grouped at the cell periphery (Fig. 7B,C). To explore the functional consequences of the podosome belt disorganization induced by tensin 3 knockdown, we performed mineralized matrix dissolution assays, incubating osteoclasts transfected with control or tensin 3 siRNA on calcium phosphate substrate. As compared to control siRNA, the transfection of tensin 3 siRNA markedly inhibited osteoclast activity (Fig. 7D). Similar results were found using a second siRNA against tensin 3 as well as two siRNAs against Dock5 (Fig. 7E).

The activity of Rho GTPases is tightly regulated in osteoclasts, and increasing or decreasing either Rac or RhoA activity is equally deleterious on the podosome belt (Ory et al., 2000), whereas dissolution of the podosome belt upon osteoclast migration is accompanied by increased activity of Rac and RhoA (Fukuda et al., 2005; Kim et al., 2006; Sakai et al., 2006). We found that tensin 3 siRNA strongly increased the global activity of RhoA (Fig. 8A). By contrast, we found a moderate increase in the global activity of Rac (Fig. 8B). Because Rac1 is enriched at the podosome belt (Fig. S4) (Sun et al., 2005; Nagai et al., 2013), the silencing of tensin 3, by disorganizing the podosome belt, might lead to its ectopic activation by various exchange factors that are expressed in osteoclasts such as Dock5, Vav3, Tiam1 or FARP2 (Brazier et al., 2006). Finally, we did not find any effect of tensin 3 silencing on the acetylation of microtubules (Fig. 8C), a marker of microtubule stability, which is also important for the regulation of the podosome belt (Biosse Duplan et al., 2014). These results show that the depletion of tensin 3 disrupts podosome patterning associated with reduced osteoclast activity and increased global levels of RhoA activity.

Taken together, our data identify tensin 3 as a new regulator of bone resorption by osteoclasts. Tensin 3 participates in the organization of podosomes and can activate Dock5, an exchange factor for the GTPase Rac, which we identified previously as a regulator of osteoclast adhesion and activity (Vives et al., 2011, 2015).

DISCUSSION

Podosome organization in osteoclasts is a major determinant of their ability to degrade the bone matrix: the formation of the podosome belt is necessary ensure efficient extracellular medium acidification to dissolve hydroxyapatite and render bone proteins amenable for degradation by proteases. We reported previously that Dock5, an activator of the GTPase Rac, participates in osteoclast podosome organization and is essential for bone resorption (Vives et al., 2011). We also showed that systemic injection of a small chemical compound that targets Dock5 exchange activity can prevent pathological bone loss in the mouse, whereas bone formation is preserved (Vives et al., 2015). We performed proteomic analysis of Dock5 partners in osteoclasts to investigate further the molecular mechanisms controlling podosome patterning in osteoclasts and, hence, bone resorption. This approach led to the identification of tensin 3 as a new regulator of osteoclast activity, which stimulates Dock5 exchange activity towards Rac. We also provide here the first analysis of podosome belt components using 3D-SIM super resolution microscopy and revealed the differential distribution of Dock5, tensin 3 and vinculin in the z-axis.

Tensin proteins (tensin 1, 2 and 3, and the short protein tensin 4) are known regulators of cell adhesion. These adaptor proteins connect integrins to the actin cytoskeleton and they can interact with the cytoplasmic tail of β-integrins at focal adhesions (Lo, 2004). Tensins are absent from nascent focal adhesions and are enriched in fibrillar adhesions (Zamir et al., 1999). Tensin 1 (Tns1), which was initially identified in chicken, has been shown to colocalize with vinculin and to surround cortactin at the podosome belt of chicken osteoclasts (Hiura et al., 1995). Since then, a report mentions the absence of tensin in the podosomes of non-invasive squamous cell carcinoma cell line UT-SCC-43A (Takkunen et al., 2010). Here, we identified tensin 3 as a partner of Dock5 in osteoclasts. We found that, as for Dock5, tensin 3 does not associate with individual podosomes in osteoclasts but that both proteins become enriched when podosomes organize into osteoclast-characteristic superstructures. Consistent with our findings, tensins have not been found as part of isolated podosomes. In agreement with previous reports (Qian et al., 2009), we found that GFP-tagged tensin 3 accumulated at focal adhesions of NIH3T3 cells. By contrast, Dock5 showed a spread localization throughout the cell (Fig. S2B). This suggests that although tensin 3 can participate in the regulation of focal adhesions, Dock5 and its presence in a complex with tensin 3 are specific for podosome-based adhesion super-structures that are typical of osteoclasts. Tensin recruitment is a feature of maturation into focal adhesions (Vicente-

Journal of Cell Science (2016) 129, 3449-3461 doi:10.1242/jcs.184622

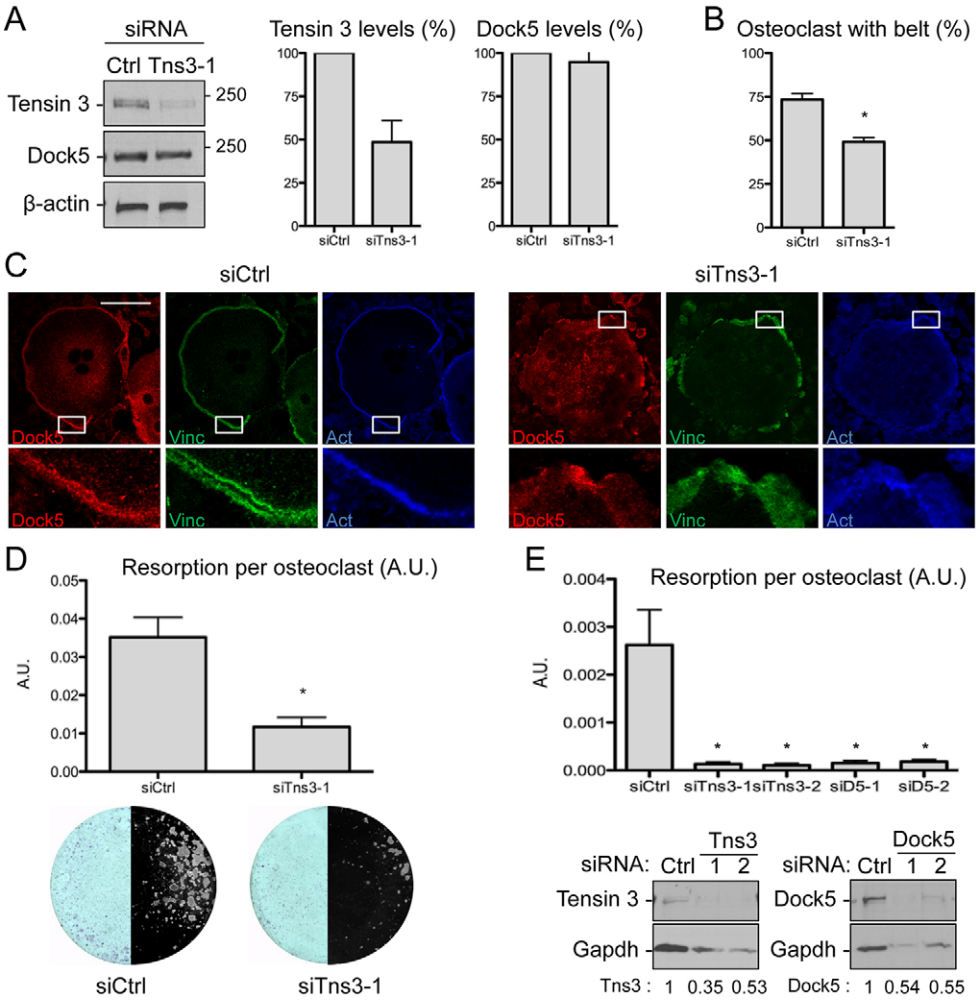

Fig. 7. Silencing of tensin 3 perturbs the podosome belt and inhibits osteoclast activity. (A) Efficiency of tensin 3 siRNA (siTns3-1) as compared to control luciferase siRNA (siCtrl), and the effect on Dock5 expression in BMM-derived osteoclasts. Bar graphs showing mean±s.e.m. values for the densitometric analysis of tensin 3 and Dock5 normalized to the levels of β-actin from three independent experiments as exemplified in the western blot. Values are percentages relative to protein levels in siCtrl-treated osteoclasts, arbitrarily set to 100%. (B) Bar graph showing the percentage of BMM-derived osteoclasts presenting a podosome belt after treatment with siCtrl or siTns3-1, from four independent experiments counting over 1800 osteoclasts, **P*<0.05 (Mann–Whitney test). (C) Confocal image of a representative BMM-derived osteoclast differentiated on glass coverslips, showing a podosome belt after siCtrl treatment or not showing a podosome belt after siTns3-1 treatment, and labeled for Dock5 (red) vinculin (Vinc, green) and actin (Act, blue). Bottom panels are magnification of the boxed areas in upper panels. Scale bar: 50 µm. (D) Bar plot graph showing the mean±s.e.m. mineral dissolution activity of BMM-derived osteoclasts treated with siCtrl or siTns3-1, determined after von Kossa staining of calcium phosphate matrices (bottom, black and white) and normalized to osteoclast numbers determined after TRAP staining (bottom, pink over blue background). **P*<0.05 (Mann–Whitney test), *n*=4 wells per condition. (E) Bar graph showing the mean±s.e.m. mineral dissolution activity of BMM-derived osteoclasts treated with siCtrl, tensin 3 (siTns3-1 or siTns3-2) or Dock5 (siD5-1 or siD5-2) siRNAs. **P*<0.05 relative to control siRNA (Kruskal–Wallis test), *n*=4 wells per condition. Bottom panels show the knockdown efficiency of tensin 3 and Dock5 proteins relative to Gapdh in the same osteoclasts, as determined by western blotting.

Manzanares et al., 2005), whereas the role of tensins in podosome-based structures has not yet been characterized. As adaptor proteins, they might organize molecular complexes essential for podosome patterning. Our results suggest that, with Dock5, tensin 3 could participate in the organization of podosome into superstructures in the osteoclast. Consistent with this idea, tensin 3 can interact with p130Cas (Qian et al., 2009), another known regulator of podosome belt formation in osteoclasts (Nagai et al., 2013) that is regulated by Dock5 (Vives et al., 2011).

Tensin-3-specific functions are not yet well understood. In particular, its role in cell migration and invasion remains controversial. In fact, tensin 3 has been described as a tumor suppressor and as an inhibitor of cell migration (Katz et al., 2007; Martuszewska et al., 2009), but tensin 3 can also be an activator of cell migration and a promoter of invasion (Qian et al., 2009; Cao et al., 2015). At the molecular level, the function of tensins is also a matter of debate. The SH2-PTB domain of tensins can bind and inhibit Dlc-family RhoGAPs (Shih et al., 2015) whereas, the ABD of tensin 3 has been shown to stimulate the RhoGAP activity by relieving Dlc1 intramolecular inhibition mediated by its N-terminal SAM domain (Cao et al., 2012). Upon EGF or PDGF stimulation, tensin 3 can also associate with phosphoinositide 3-kinase (PI3K) and promote Rac activation at the leading edge of the cell (Cao et al., 2015). Therefore the adaptor protein tensin 3 appears to be a versatile regulator of RhoGTPase signaling pathways. We found that Dock5 exchange activity is repressed by its N-terminal SH3 domain, consistent with what was reported previously for Dock1 (Lu et al., 2005). We show here that tensin 3 can potentiate Dock5

Journal of Cell Science (2016) 129, 3449-3461 doi:10.1242/jcs.184622

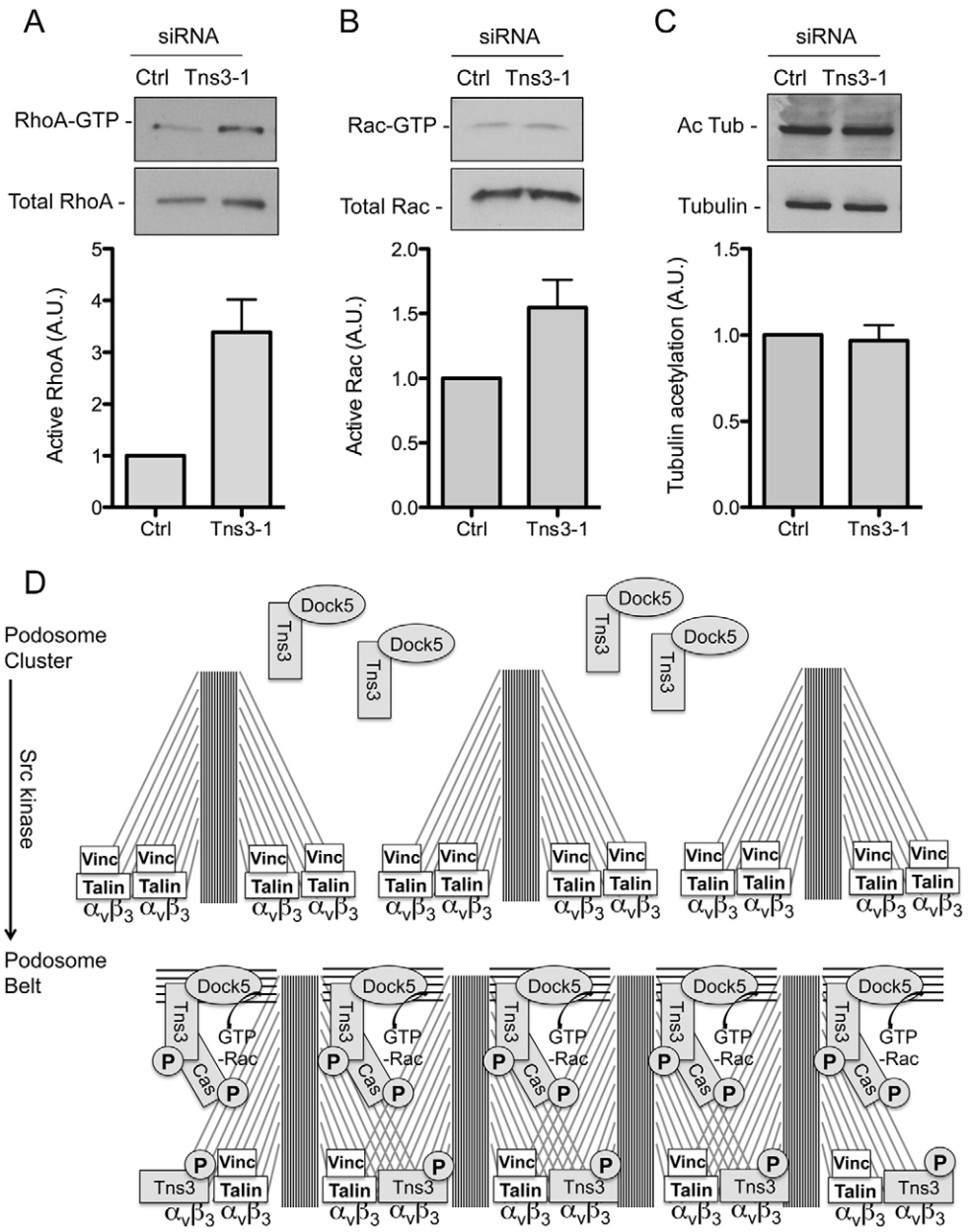

Fig. 8. Silencing of tensin 3 strongly increases RhoA activity. (A,B) Representative pulldown assay to determine the levels of active RhoA and Rac in osteoclasts treated with control (Ctrl) or tensin 3 (Tns3-1) siRNAs. Bar graphs show the mean±s.e.m. levels of active RhoA (n=4) and Rac (n=4) normalized to the total levels of the GTPase as determined by densitometric analysis. (C) Representative western blot to determine the levels of acetylated tubulin (Ac Tub) relative to total tubulin in osteoclasts treated as in A and B. Bar graph shows the show the mean±s.e.m. levels of acetylated tubulin normalized to the total levels of tubulin (n=7) as determined by densitometric analysis. (D) A proposed model for tensin 3 and Dock5 recruitment upon podosome belt formation triggered by Src. Phosphorylation of tensin 3 by Src allows its recruitment to β3 integrin and its interaction with p130Cas at podosomes. This allows the concentration of the Dock5–tensin-3 complex at the podosomes to allow local activation of Rac, thereby triggering the formation of actin fibers that interconnect individual podosomes to form the podosome belt.

exchange activity towards Rac. We also found that tensin 3 is necessary for the correct patterning of osteoclast podosomes, which is known to also require Dock5 (Vives et al., 2011), Rac (Razzouk et al., 1999; Wang et al., 2008; Croke et al., 2011) and the activation of Rac by Dock5 (Vives et al., 2015).

We show that the N-terminal region of Dock5 can interact with the ABD of tensin 3. Nevertheless, only full-length tensin 3 could stimulate Dock5 activity, suggesting that, as in the case of Dlc1 (Shih et al., 2015), the functional interaction between tensin 3 and Dock5 is complicated. The activation of Dock5 by tensin 3 might involve conformational cues provided by full-length tensin 3 as well as other partners of the protein, which would need more extensive investigation. By contrast, we found that deletion of tensin 3 in osteoclasts led to a strong activation of RhoA and a mild activation of Rac, similar to what was reported in MCF10A cells (Cao et al., 2015). This suggests that tensin 3 regulates other signaling pathways in osteoclasts, possibly involving Dlc RhoGAP proteins and/or its other partner β3 integrin. Extending the study of the functional interaction between tensins and Dock proteins in relevant cellular systems would indicate whether our observations on tensin 3 and Dock5 could be generalized to more members of the tensin and Dock protein families, and to other adhesion structures such as focal adhesions.

Tensin 3 and Dock5 concomitantly enrich in podosome rings and show very condensed labeling at the podosome belt. At the osteoclast podosome belt, classical confocal microcopy revealed a colocalization of tensin 3, Dock5 and vinculin flanking the podosome cores. Using 3D-SIM super-resolution microscopy, we could reveal differential localization of the three proteins along the z-axis. Dock5 appeared to colocalize with tensin 3 rather than with vinculin, with Dock5 standing preferentially above the vinculin layer, whereas tensin 3 appeared to have a broader distribution. Consistently, we found that, in osteoclasts, tensin 3 could associate with both β3 integrin, which relied on Src activity, and to Dock5, in a manner not dependent on Src activity. Of note, another partner of β3 integrin is talin, which is part of the cloud of isolated podosomes (Meddens et al., 2014) but it is only weakly

enriched at the podosome belt (Zou et al., 2013). Phosphorylation of β-integrin tail by Src has been shown to displace talin and allow the binding of tensin (McCleverty et al., 2007). Taking these observations together, one could speculate that during podosome patterning, which is Src dependent (Destaing et al., 2008), tensin 3 molecules could functions as a bridge to connect the β3 integrin layer and Dock5 within the above acto-myosin layer, which runs between podosomes (Linder and Wiesner, 2015). This would allow podosomes to get closer to one another upon their patterning into rings and the belt (Luxenburg et al., 2007). Within the acto-myosin network interconnecting podosomes, tensin 3 would allow the optimal activation of Dock5 and then of Rac, to ensure the correct organization of podosomes and the efficient function of osteoclasts (Fig. 8D).

Our study identifies the adhesion regulator tensin 3 as a new player in the cytoskeleton organization and in the bone resorption activity of osteoclasts. The expression of both Dock5 and tensin 3 is induced during osteoclast differentiation. Their interaction in osteoclasts, their concomitant recruitment at podosome superstructures, their colocalization at the podosome belt and the fact that tensin 3 can relieve the intra-molecular inhibition of Dock5 exchange activity suggests that the interaction between tensin 3 and Dock5 could promote the local activation of Rac, which is also enriched at the podosome belt, for proper podosome patterning. Similar to the role of tensins in focal adhesion maturation and stabilization, our findings suggest that tensin 3 could function as a regulator of podosome-based adhesion maturation, during which the highly dynamic individual podosomes get compacted into a belt, a stable superstructure necessary for the long process of bone degradation.

MATERIALS AND METHODS

Mice

4-week-old C57Bl/6J were purchased from Harlan France and maintained in the animal facilities of the CNRS in Montpellier, France. Procedures involving mice were performed in compliance with local animal welfare laws, guidelines and policies, according to the rules of the regional ethical committee.

Reagents and plasmids

The siRNAs were purchased as siRNA duplexes from Eurogentec. The sequences were: siTns3-1, 5′-GGUUUGCAAUGAAGAAGUU-3′, according to Qian et al. (2009), and siTns3-si2, 5′-GAGUGGUCAUAU-CGUCCUACA-3′, for tensin3; siD5-1, 5′-GGAGCUCACAAACACGC-UACG-3′, and siD5-2, 5′-AGUCAUAGCUGCAAAGGAAGU-3′, for Dock5, according to short hairpin RNAs (shRNAs) used in Brazier et al. (2006) and Vives et al. (2011); and Cy5-labeled control siCtrl, 5′-CUUACGCUGAGUACUUCGA-3′, targeting luciferase, according to Knoch et al. (2004). Full-length tensin 3 coding sequence was purchased as a synthetic gene in pDONR221 entry vector from Fisher Scientific and transferred by Gateway recombination into acceptor eukaryotic cell expression vectors with N-terminal GFP (peGFPC3 RfC) or Myc (pCDNA3 MycS1 RfC) tagging. Tensin 3 deletion mutants were further subcloned in pEGFP. Full-length Dock5 and deletion constructs of Dock5 were cloned in pCMV5 with a Flag tag at the N-terminal end or in pEGFP-C. The pEBB vecors encoding Flag-tagged full-length and ΔT625 Elmo were a gift from Kodimangalam S. Ravichandran (University of Virginia, Charlottesville, VA). Other constructs were as described elsewhere (Brazier et al., 2006; Vives et al., 2011). Antibody recognizing Dock5 C-terminus was as described and characterized before and used as described in Table S3 (Laurin et al., 2008; Vives et al., 2011). All other antibodies were commercial, they were used as described in Table S3.

Osteoclast preparation

RAW264.7 cells stably expressing GFP were obtained as described from a pMxS-puro vector expressing GFP (Brazier et al., 2009). To prepare RAW264.7 cells stably expressing GFP–Dock5, cells were transfected with pEFGP vector expressing GFP–Dock5 (Vives et al., 2011) using siImporter (Millopore) and selected for GFP-positive cells with 300 µg/ml G418. To obtain osteoclasts, RAW264.7 cells were then grown for 4 to 5 days with RANKL (50 ng/ml).

Primary osteoclasts were obtained from mouse bone marrow as described previously (Brazier et al., 2006; Vives et al., 2011). Briefly, BMMs were obtained from long bones of 6- to 8-week-old C57BL/6J mice by growing non-adherent cells for 24 h in α-MEM supplemented with 10% heat-inactivated fetal calf serum and 2 mM glutamine and 30 ng/ml M-CSF (Peprotech), and osteoclasts were differentiated by culturing BMMs in α-MEM supplemented with 10% heat-inactivated fetal calf serum and 2 mM glutamine with RANKL (100 ng/ml) and M-CSF (30 ng/ml) (Peprotech) for 5 days. For siRNA treatments, cells were transfected for 4 h in Gibco OptiMEM medium (Thermofisher) with 100 nM siRNA using siImporter (Millipore), according to the manufacturer's instructions, at day 0 and day 3 of differentiation. Protein knockdown was measured on whole-cell extracts by western blotting with anti-Dock5 or anti-tensin 3 antibodies and normalized to Gapdh or β-actin expression. Quantification was performed with Image J 1.4.7v software.

Proteomic identification of Dock5 partners

RAW264.7-cell-derived osteoclasts expressing GFP or GFP–Dock5 were differentiated in 10-cm plates. Whole-cell extracts were prepared in 400 µl cold extraction buffer (50 mM Tris-HCl pH 7.5, 120 mM NaCl, 1 mM EDTA, 6 mM EGTA, 1 mM Benzamidine, 1% IGEPAL, 20 mM NaF, 0.5 mM Na_3VO_4, 15 mM p-Nitrophenyl Phosphate with Sigma protease inhibitory cocktail) per plate. Eight plates were used for each sample. Lysates were cleared by centrifugation for 10 min at 14,000 ***g***. Immunoprecipitation of GFP-tagged proteins was performed by a 1-h incubation with anti-GFP VHH antibody covalently coupled to agarose beads (GFP-Trap®-A, ChromoTek) at 1:100 (v/v) of cleared protein extract, followed by three washes in extraction buffer.

Bound proteins were recovered by boiling the beads in 1× Laemmli buffer and separated on a 12% denaturing SDS-PAGE acrylamide gel. Gel lanes were sliced into 13 equal gel pieces; proteins were digested in-gel using trypsin (600 ng/band, Gold, Promega). Digested products were dehydrated in a vacuum centrifuge. The generated peptides were analyzed online by nano-flow HPLC–nanoelectrospray ionization using an LTQ Orbitrap Xl mass spectrometer (Thermo Fisher Scientific) coupled to an Ultimate 3000 HPLC (Dionex, Thermo Fisher Scientific). Desalting and pre-concentration of samples was performed on-line on a Pepmap® pre-column (0.3 mm×10 mm, Dionex). A gradient consisting of 0–40% solution B in solution A for 60 min, followed by 80% solution B and 20% solution A for 15 min (solution A, 0.1% formic acid and 2% acetonitrile in water; solution B, 0.1% formic acid in acetonitrile) at 300 nl/min was used to elute peptides from the capillary reverse-phase column (0.075 mm×150 mm, Pepmap®, Dionex). Eluted peptides were electrosprayed online at a voltage of 2.2 kV into an LTQ Orbitrap Xl mass spectrometer. A cycle of one full-scan mass spectrum (400–2000 *m*/*z*) at a resolution of 60,000 (at 400 *m*/*z*) in the orbitrap, followed by five data-dependent MS/MS spectra was repeated continuously throughout the nanoLC separation. All MS/MS spectra (acquired using the linear trap quadrupole) were recorded using normalized collision energy (35%, activation Q 0.25 and activation time 30 ms) with an isolation window of 3 *m*/*z*. Data were acquired using the Xcalibur software (v 2.1).

All MS/MS spectra were searched against the *Mus musculus* entries of either SwissProt or TrEMBL databases (http://www.uniprot.org/) using the Proteome Discover software v 1.2 (Thermo Fisher Scientific) and Mascot v 2.3 algorithm (http://www.matrixscience.com/) with trypsin enzyme specificity and one trypsin-missed cleavage. Carbamidomethylation was set as fixed cystein modification and oxidation was set as variable methionine modification for searches. A peptide mass tolerance or 5 ppm and a fragment mass tolerance of 0.5 Da were allowed for identification. Management and validation of mass spectrometry data were carried out using Proteome Discoverer software v 1.2 ($P<0.01$ for 2 peptides or more per protein).

The abundance of the proteins associated with GFP or GFP–Dock5 was defined as the average number of peptide-spectrum match (PSM) in the immunoprecipitates of extracts from osteoclasts expressing GFP ($n=2$

independent differentiation experiments) or GFP–Dock5 (n=3 independent differentiation experiments).

Confocal microscope imaging

Osteoclasts were fixed with fixation buffer (3.6% paraformaldehyde in Pipes 60 mM, Hepes 25 mM, EGTA 10 mM, $MgSO_4$ 4 mM, pH 6.9) for 10 min and permeabilized for 1 min with 0.1% Triton X-100 in PBS. Indirect immunofluorescence was performed after saturation with 1% BSA in PBS for 15 min, followed by incubation with appropriated primary antibodies in PBS containing 1% BSA during 1 h. After three washes in PBS, primary antibodies were revealed with appropriate Alexa-Fluor-conjugated antiantibodies. Alexa-Fluor-633-conjugated phalloidin was used to reveal F-actin, and cells were mounted in CitiFluor Tris MWL 4-88 mounting medium (Biovalley). Images were acquired using an SP5 confocal microscope (Leica), each channel was imaged sequentially using the multitrack recording module before merging to ensure only one fluorochrome was detected at a time. Images were acquired with MetaMorph 7.7.6 software and mounted in Adobe Photoshop CS5. Dock5 and tensin 3 localization relative to vinculin and actin in podosome belt, rings and clusters, were determined from four osteoclasts differentiations examining at least 100 osteoclasts per experiment.

3D structured illumination microscopy

Osteoclasts were cultured on high precision no. 1.5H glass coverslips (Marienfeld GmbH), and fixed and processed for immunofluorescence as above. To reveal the primary antibodies, we used the following secondary antibodies: donkey Alexa-Fluor-488-conjugated anti-rabbit-IgG and Alexa-Fluor-568-conjugated anti-goat-IgG antibodies or goat Alexa-Fluor-568-conjugated anti-mouse-IgG antibody (Life Technologies). CF405M conjugated phalloidin was used to label actin (Biotium). Samples were mounted using Prolong Gold (Life Technologies). 3D-SIM imaging was performed using an OMX-V3 microscope (General Electrics) equipped with 405-nm, 488-nm and 561-nm lasers and the corresponding dichroic and filter sets. Reconstruction and alignment of the 3D-SIM images was carried out with softWoRx v 5.0 (General Electrics). 100-nm green fluorescent beads (Life Technologies) were used to measure the optical transfer function (otf) used for the 405 and 488 channels, and 100-nm red fluorescent beads (Life Technologies) were used to measure the otf used for the 561 channel. 170-nm TetraSpeck beads (Life Technologies) were employed to measure the offsets and rotation parameters used in the image registration. Reconstructed 3D-SIM images were analyzed using Image J 1.4.7v software.

Active Rac1 and RhoA quantification

GTP-bound Rac1 was pulled down from HEK293T and osteoclast cell extracts using GST-fused PAK1 CRIB domain, as described previously (Vives et al., 2011, 2015), and revealed by western blotting with anti-Rac1 antibodies. Active Rac1 was normalized to total Rac1 and to Dock5 expression as determined by western blotting on the corresponding whole-cell extracts. Quantification was performed with Image J 1.4.7v software. GTP-bound RhoA was pulled down from osteoclast extracts using GST–Rhotekin–RBD beads according to the manufacture's instructions (Cytoskeleton).

Detection of mineral dissolution by osteoclasts

To measure the mineral dissolution activity of osteoclasts, osteoclasts were scrapped in PBS containing 0.025 mM EDTA at day 4 of differentiation (24 h after the second siRNA transfection) and seeded for 3 days onto inorganic crystalline calcium phosphate (CaP)-coated multiwells (Osteo Assay Surface, Corning). In each experiment, four wells were then stained for TRAP activity to count osteoclasts and four wells with Von Kossa stain to measure CaP dissolution as described previously (Vives et al., 2011). Von Kossa and TRAP staining were observed with a Nikon SMZ1000 stereomicroscope and images were acquired with a Nikon DXM 1200F CCD camera. Quantification was done with Image J 1.4.7v software.

Immunoprecipitation and western blotting

Osteoclasts and HEK293T cells were lysed in lysis buffer (50 mM Tris-HCl pH 7.5, 120 mM NaCl, 1 mM EDTA, 6 mM EGTA, 1% NP-40, 20 mM NaF, 100 µM Na_3VO_4) and directly separated in a denaturing SDS-PAGE acrylamide gel or first submitted to immunoprecipitation and analyzed by western blotting with the appropriate antibodies. Proteins of interest were visualized by the ECL Western Lightning Plus detection system (Perkin Elmer) with horseradish-peroxidase-conjugated secondary antibodies (GE Healthcare) and quantified using Image J 1.4.7v software.

Statistical analyses

We assessed statistical significance with the non-parametric statistical tests as mentioned in the corresponding figure legends. All analyses were performed using GraphPad Prism (GraphPad Software, Inc., La Jolla, CA). $P<0.05$ was considered statistically significant.

Acknowledgements

The authors wish to thank Edith Demettre (Pôle Protéome de Montpellier) and Perrine Suère (CRBM, Montpellier) for technical assistance, and Virginie Vives (CRBM Montpellier) for helpful discussions and critical reading of the manuscript.

Competing interests

The authors declare no competing or financial interests.

Author contributions

A.B. designed the research. H.T. and A.M. designed and performed most of the experiments. A.B. and H.T. wrote the paper. S.U. performed proteomic result analyses. J.M.-L. supervised the 3D-SIM acquisition and processing by H.T. H.T. and S.d.R. analyzed fluorescence images. All contributors discussed the results and commented on the manuscript.

Funding

This work was supported by research grants from the Institut National du Cancer [grant number INCa-4361 to A.B.]; the Agence Nationale de la Recherche (ANR) [grant number ANR-2011-BLAN-006 to A.B.]; the Société Française de Rhumatologie (SFR) [grant number 2676 to A.B.]; and the Ligue Contre le Cancer [grant number TABY12312].

Supplementary information

Supplementary information available online at
http://jcs.biologists.org/lookup/doi/10.1242/jcs.184622.supplemental

References

Biosse Duplan, M., Zalli, D., Stephens, S., Zenger, S., Neff, L., Oelkers, J. M., Lai, F. P. L., Horne, W., Rottner, K. and Baron, R. (2014). Microtubule dynamic instability controls podosome patterning in osteoclasts through EB1, cortactin, and Src. *Mol. Cell. Biol.* **34**, 16-29.

Brazier, H., Stephens, S., Ory, S., Fort, P., Morrison, N. and Blangy, A. (2006). Expression profile of RhoGTPases and RhoGEFs during RANKL-stimulated osteoclastogenesis: identification of essential genes in osteoclasts. *J. Bone Miner. Res.* **21**, 1387-1398.

Brazier, H., Pawlak, G., Vives, V. and Blangy, A. (2009). The Rho GTPase Wrch1 regulates osteoclast precursor adhesion and migration. *Int. J. Biochem. Cell Biol.* **41**, 1391-1401.

Cao, X., Voss, C., Zhao, B., Kaneko, T. and Li, S. S.-C. (2012). Differential regulation of the activity of deleted in liver cancer 1 (DLC1) by tensins controls cell migration and transformation. *Proc. Natl. Acad. Sci. USA* **109**, 1455-1460.

Cao, X., Kaneko, T., Li, J. S., Liu, A.-D., Voss, C. and Li, S. S. C. (2015). A phosphorylation switch controls the spatiotemporal activation of Rho GTPases in directional cell migration. *Nat. Commun.* **6**, 7721.

Croke, M., Ross, F. P., Korhonen, M., Williams, D. A., Zou, W. and Teitelbaum, S. L. (2011). Rac deletion in osteoclasts causes severe osteopetrosis. *J. Cell Sci.* **124**, 3811-3821.

Destaing, O., Saltel, F., Géminard, J.-C., Jurdic, P. and Bard, F. (2003). Podosomes display actin turnover and dynamic self-organization in osteoclasts expressing actin-green fluorescent protein. *Mol. Biol. Cell* **14**, 407-416.

Destaing, O., Sanjay, A., Itzstein, C., Horne, W. C., Toomre, D., De Camilli, P. and Baron, R. (2008). The tyrosine kinase activity of c-Src regulates actin dynamics and organization of podosomes in osteoclasts. *Mol. Biol. Cell* **19**, 394-404.

Faccio, R., Teitelbaum, S. L., Fujikawa, K., Chappel, J., Zallone, A., Tybulewicz, V. L., Ross, F. P. and Swat, W. (2005). Vav3 regulates osteoclast function and bone mass. *Nat. Med.* **11**, 284-290.

Fukuda, A., Hikita, A., Wakeyama, H., Akiyama, T., Oda, H., Nakamura, K. and Tanaka, S. (2005). Regulation of osteoclast apoptosis and motility by small GTPase binding protein Rac1. *J. Bone Miner. Res.* **20**, 2245-2253.

Fukunaga, T., Zou, W., Warren, J. T. and Teitelbaum, S. L. (2014). Vinculin regulates osteoclast function. *J. Biol. Chem.* **289**, 13554-13564.
Gadea, G. and Blangy, A. (2014). Dock-family exchange factors in cell migration and disease. *Eur. J. Cell Biol.* **93**, 466-477.
Georgess, D., Machuca-Gayet, I., Blangy, A. and Jurdic, P. (2014). Podosome organization drives osteoclast-mediated bone resorption. *Cell Adh. Migr.* **8**, 192-204.
Gil-Henn, H., Destaing, O., Sims, N. A., Aoki, K., Alles, N., Neff, L., Sanjay, A., Bruzzaniti, A., De Camilli, P., Baron, R. et al. (2007). Defective microtubule-dependent podosome organization in osteoclasts leads to increased bone density in Pyk2(-/-) mice. *J. Cell Biol.* **178**, 1053-1064.
Hiura, K., Lim, S.-S., Little, S. P., Lin, S. and Sato, M. (1995). Differentiation dependent expression of tensin and cortactin in chicken osteoclasts. *Cell Motil. Cytoskeleton* **30**, 272-284.
Katz, M., Amit, I., Citri, A., Shay, T., Carvalho, S., Lavi, S., Milanezi, F., Lyass, L., Amariglio, N., Jacob-Hirsch, J. et al. (2007). A reciprocal tensin-3–cten switch mediates EGF-driven mammary cell migration. *Nat. Cell Biol.* **9**, 961-969.
Kim, H.-J., Zhao, H., Kitaura, H., Bhattacharyya, S., Brewer, J. A., Muglia, L. J., Ross, F. P. and Teitelbaum, S. L. (2006). Glucocorticoids suppress bone formation via the osteoclast. *J. Clin. Invest.* **116**, 2152-2160.
Knoch, K.-P., Bergert, H., Borgonovo, B., Saeger, H.-D., Altkrüger, A., Verkade, P. and Solimena, M. (2004). Polypyrimidine tract-binding protein promotes insulin secretory granule biogenesis. *Nat. Cell Biol.* **6**, 207-214.
Komander, D., Patel, M., Laurin, M., Fradet, N., Pelletier, A., Barford, D. and Cote, J.-F. (2008). An alpha-helical extension of the ELMO1 pleckstrin homology domain mediates direct interaction to DOCK180 and is critical in Rac signaling. *Mol. Biol. Cell* **19**, 4837-4851.
Laurin, M., Fradet, N., Blangy, A., Hall, A., Vuori, K. and Cote, J.-F. (2008). The atypical Rac activator Dock180 (Dock1) regulates myoblast fusion in vivo. *Proc. Natl. Acad. Sci. USA* **105**, 15446-15451.
Linder, S. and Wiesner, C. (2015). Tools of the trade: podosomes as multipurpose organelles of monocytic cells. *Cell. Mol. Life Sci.* **72**, 121-135.
Lo, S. H. (2004). Tensin. *Int. J. Biochem. Cell Biol.* **36**, 31-34.
Lu, M., Kinchen, J. M., Rossman, K. L., Grimsley, C., Hall, M., Sondek, J., Hengartner, M. O., Yajnik, V. and Ravichandran, K. S. (2005). A Steric-inhibition model for regulation of nucleotide exchange via the Dock180 family of GEFs. *Curr. Biol.* **15**, 371-377.
Luxenburg, C., Geblinger, D., Klein, E., Anderson, K., Hanein, D., Geiger, B. and Addadi, L. (2007). The architecture of the adhesive apparatus of cultured osteoclasts: from podosome formation to sealing zone assembly. *PLoS ONE* **2**, e179.
Makino, Y., Tsuda, M., Ichihara, S., Watanabe, T., Sakai, M., Sawa, H., Nagashima, K., Hatakeyama, S. and Tanaka, S. (2006). Elmo1 inhibits ubiquitylation of Dock180. *J. Cell Sci.* **119**, 923-932.
Martuszewska, D., Ljungberg, B., Johansson, M., Landberg, G., Oslakovic, C., Dahlbäck, B. and Hafizi, S. (2009). Tensin3 is a negative regulator of cell migration and all four Tensin family members are downregulated in human kidney cancer. *PLoS ONE* **4**, e4350.
McCleverty, C. J., Lin, D. C. and Liddington, R. C. (2007). Structure of the PTB domain of tensin1 and a model for its recruitment to fibrillar adhesions. *Protein Sci.* **16**, 1223-1229.
Meddens, M. B. M., van den Dries, K. and Cambi, A. (2014). Podosomes revealed by advanced bioimaging: what did we learn? *Eur. J. Cell Biol.* **93**, 380-387.
Nagai, Y., Osawa, K., Fukushima, H., Tamura, Y., Aoki, K., Ohya, K., Yasuda, H., Hikiji, H., Takahashi, M., Seta, Y. et al. (2013). p130Cas, Crk-associated substrate, plays important roles in osteoclastic bone resorption. *J. Bone Miner. Res.* **28**, 2449-2462.
Ory, S., Munari-Silem, Y., Fort, P. and Jurdic, P. (2000). Rho and Rac exert antagonistic functions on spreading of macrophage-derived multinucleated cells and are not required for actin fiber formation. *J. Cell Sci.* **113**, 1177-1188.
Ory, S., Brazier, H., Pawlak, G. and Blangy, A. (2008). Rho GTPases in osteoclasts: orchestrators of podosome arrangement. *Eur. J. Cell Biol.* **87**, 469-477.
Qian, X., Li, G., Vass, W. C., Papageorge, A., Walker, R. C., Asnaghi, L., Steinbach, P. J., Tosato, G., Hunter, K. and Lowy, D. R. (2009). The Tensin-3 protein, including its SH2 domain, is phosphorylated by Src and contributes to tumorigenesis and metastasis. *Cancer Cell* **16**, 246-258.
Razzouk, S., Lieberherr, M. and Cournot, G. (1999). Rac-GTPase, osteoclast cytoskeleton and bone resorption. *Eur. J. Cell Biol.* **78**, 249-255.
Sakai, H., Chen, Y., Itokawa, T., Yu, K.-P., Zhu, M.-l. and Insogna, K. (2006). Activated c-Fms recruits Vav and Rac during CSF-1-induced cytoskeletal remodeling and spreading in osteoclasts. *Bone* **39**, 1290-1301.
Saltel, F., Destaing, O., Bard, F., Eichert, D. and Jurdic, P. (2004). Apatite-mediated actin dynamics in resorbing osteoclasts. *Mol. Biol. Cell* **15**, 5231-5241.
Shih, Y.-P., Sun, P., Wang, A. and Lo, S. H. (2015). Tensin1 positively regulates RhoA activity through its interaction with DLC1. *Biochim. Biophys. Acta* **1853**, 3258-3265.
Sun, Y., Buki, K. G., Ettala, O., Vaaraniemi, J. P. and Vaananen, H. K. (2005). Possible role of direct Rac1-Rab7 interaction in ruffled border formation of osteoclasts. *J. Biol. Chem.* **280**, 32356-32361.
Takegahara, N., Kang, S., Nojima, S., Takamatsu, H., Okuno, T., Kikutani, H., Toyofuku, T. and Kumanogoh, A. (2010). Integral roles of a guanine nucleotide exchange factor, FARP2, in osteoclast podosome rearrangements. *FASEB J.* **24**, 4782-4792.
Takkunen, M., Hukkanen, M., Liljeström, M., Grenman, R. and Virtanen, I. (2010). Podosome-like structures of non-invasive carcinoma cells are replaced in epithelial-mesenchymal transition by actin comet-embedded invadopodia. *J. Cell Mol. Med.* **14**, 1569-1593.
Teitelbaum, S. L. and Ross, F. P. (2003). Genetic regulation of osteoclast development and function. *Nat. Rev. Genet.* **4**, 638-649.
Touaitahuata, H., Blangy, A. and Vives, V. (2014a). Modulation of osteoclast differentiation and bone resorption by Rho GTPases. *Small GTPases* **5**, e28119.
Touaitahuata, H., Cres, G., de Rossi, S., Vives, V. and Blangy, A. (2014b). The mineral dissolution function of osteoclasts is dispensable for hypertrophic cartilage degradation during long bone development and growth. *Dev. Biol.* **393**, 57-70.
Vicente-Manzanares, M., Webb, D. J. and Horwitz, A. R. (2005). Cell migration at a glance. *J. Cell Sci.* **118**, 4917-4919.
Vives, V., Laurin, M., Cres, G., Larrousse, P., Morichaud, Z., Noel, D., Côté, J.-F. and Blangy, A. (2011). The Rac1 exchange factor Dock5 is essential for bone resorption by osteoclasts. *J. Bone Miner. Res.* **26**, 1099-1110.
Vives, V., Cres, G., Richard, C., Busson, M., Ferrandez, Y., Planson, A.-G., Zeghouf, M., Cherfils, J., Malaval, L. and Blangy, A. (2015). Pharmacological inhibition of Dock5 prevents osteolysis by affecting osteoclast podosome organization while preserving bone formation. *Nat. Commun.* **6**, 6218.
Wang, Y., Lebowitz, D., Sun, C., Thang, H., Grynpas, M. D. and Glogauer, M. (2008). Identifying the relative contributions of rac1 and rac2 to osteoclastogenesis. *J. Bone Miner. Res.* **23**, 260-270.
Weitzmann, M. N. and Pacifici, R. (2006). Estrogen deficiency and bone loss: an inflammatory tale. *J. Clin. Invest.* **116**, 1186-1194.
Zamir, E., Katz, B. Z., Aota, S., Yamada, K. M., Geiger, B. and Kam, Z. (1999). Molecular diversity of cell-matrix adhesions. *J. Cell Sci.* **112**, 1655-1669.
Zou, W., Izawa, T., Zhu, T., Chappel, J., Otero, K., Monkley, S. J., Critchley, D. R., Petrich, B. G., Morozov, A., Ginsberg, M. H. et al. (2013). Talin1 and Rap1 are critical for osteoclast function. *Mol. Cell. Biol.* **33**, 830-844.